applied sciences

MDPI

Article

A Contribution to Facilitate the Seismic Design in Lebanon Using Short-Length Spectrum-Consistent Earthquakes

Amal Gerges [1], Maria Cristina Porcu [1] and Juan Carlos Vielma Pérez [2,*]

[1] Department of Civil, Environmental Engineering and Architecture, University of Cagliari, Via Marengo 2, 09123 Cagliari, Italy; amal.gerges@unica.it (A.G.); mcporcu@unica.it (M.C.P.)
[2] Civil Engineering School, Pontificia Universidad Católica de Valparaíso, Valparaíso 2340000, Chile
* Correspondence: juan.vielma@pucv.cl

Abstract: Seismic regulations of developing countries are often grounded on rules of more experienced countries. The Lebanese regulations refer to four foreign codes, this excess of guidelines generating confusion and conflicting design choices. Moreover, the scarcity of earthquakes recorded in the Lebanese area makes it difficult to obtain suitable sets of spectrum-consistent accelerograms for dynamic analyses. Sorting through the reference regulations and the indications for their local application, this paper derives and compares all the design response spectra allowed by the Lebanese code. Consistent with the design response spectra of the two codes that are still in force (of the four referred to), some suites of spectrum-consistent accelerograms are derived. Based on the Arias intensity, a general procedure is also proposed to reduce the time duration of the accelerograms, while saving the earthquake energy content and, thus, the reliability of the results. Full-length and short-length spectrum-consistent accelerograms are thus made available for the Lebanese design. With reference to a two-dimensional model some comparisons between response-spectrum-based and earthquake-based analyses are provided, which showed that the Lebanese code allows different safety levels for earthquake-resistant buildings. The paper provides a very useful contribution to researchers and designers that are involved in the protection of the Lebanese building heritage from seismic hazards, and it also provides data and tools that can be more generally exploited in other seismic areas.

Keywords: Lebanese seismic design; spectrum-consistent Lebanese earthquakes; energy-saving cutting procedure; short-length accelerograms

Citation: Gerges, A.; Porcu, M.C.; Vielma Pérez, J.C. A Contribution to Facilitate the Seismic Design in Lebanon Using Short-Length Spectrum-Consistent Earthquakes. *Appl. Sci.* **2023**, *13*, 12990. https://doi.org/10.3390/app132412990

Academic Editor: Maria Favvata

Received: 2 September 2023
Revised: 1 December 2023
Accepted: 2 December 2023
Published: 5 December 2023

1. Introduction

Design response spectra (DRS) and spectrum-consistent earthquakes (SCEs) are powerful tools to design earthquake-resistant structures. According to codes, static or dynamic methods of analysis may in fact be adopted to assess the seismic performance of new or existing buildings. Some such methods are based on DRS while some others apply SCEs to perform numerical analyses. Typically, static methods derive the horizontal design loads directly from the DRS, while dynamic methods may refer either to DRS or to SCEs. Seismic methods may also be linear or non-linear, depending on whether the structural material is modelled through a linear–elastic or an elastic–plastic behavior. The simplest method proposed by codes is the linear–static one, which applies a pattern of static loads proportional to the masses and to the DRS accelerations; it generally gives less accurate results [1]. The non-linear–static method (also known as Pushover Analysis) applies a pattern of increasing static loads to the structure until targeted inelastic displacement levels are reached [2]. On the other hand, linear–dynamic methods are basically two. The first one is the Modal Response Spectrum Analysis (MRSA) which combines the maximum contributions of the most significant vibration modes of a structure as taken from the DRS. It is usually assumed to be the reference method by codes [3], and is widely adopted for the

seismic assessment of new and retrofitted buildings [4]. The second method is the Linear Time-History Analysis (LTHA), which directly integrates the linear differential motion equations of the system under SCEs. The most powerful code-compliant method to assess the seismic behavior of a structure is the Non-Linear Time-History Analysis (NLTHA), which is based on integrating the non-linear differential equations of motion under SCEs. This method can be applied to any kind of structure and material, leading to very useful results, e.g., [3,5,6]. The SCEs can be also used to perform Incremental Dynamic Analyses and to build fragility curves [7].

Since SCEs are design earthquakes which must be consistent with the DRS, all the above-mentioned methods, directly or indirectly, refer to the DRS. This means that the accurate definition of the DRS is of paramount importance both to design new earthquake-resistant buildings and to assess the seismic vulnerability of existing buildings. DRSs are provided by codes as a function of some parameters accounting for seismic hazard, geological and topographical conditions, limit states, damping ratio, behavior factors, life cycle and use categories. On the other hand, a database of recorded ground motions should be at researcher's disposal to obtain suitable suites of synthetic SCEs. Inconsistencies in codes in the definition of DRS [8,9], as well as unavailability of suitable seismic records for the dynamic analyses are some of the obstacles that may compromise the seismic design/assessment of buildings.

This kind of risk might affect the Lebanese seismic design. Crossed by an active fault which extends from the Red Sea to Turkey, Lebanon lies in an extremely important tectonic system that generated the catastrophic Kahramanmaras 2023 earthquake, mainly affecting Turkey and Syria. Lebanon introduced seismic regulations only recently [10,11]. Such regulations mostly refer to four seismic codes of foreign countries, this leading to unclear and/or conflicting instructions for the response spectrum definition. In addition, practitioners or researchers who want to carry out time-history analyses, also face the difficulty of finding suitable records of Lebanese earthquakes [12]. On the other hand, available records relevant to earthquakes occurring along other strike–slip faults, such as the San Andreas fault, have different features and are characterized by different geological mechanisms from the earthquakes affecting the Eastern Mediterranean coastal region. Thus, referring to those records may lead to inconsistent results.

This paper mainly has a twofold purpose. The first one is to derive and compare the different DRS allowed by the Lebanese code. The second purpose is to obtain suitable sets of spectrum-consistent accelerograms to be used for dynamic analyses of Lebanese structures. The matter of selecting sets of accelerograms that are compatible to given design spectra is of the utmost importance to carry out time-history seismic analyses. Many studies dealt with this matter, see e.g., [13–18], and most codes provide rules and suggestions for this purpose. A recent paper proposed a site-specific estimation of strong ground motions in the Lebanese area [19], and also showed that the Lebanese norm may give unsafe amplification factors for short period structures. In [20], a probabilistic study of the Lebanese seismic hazard was performed to provide design requirements.

Two main issues should be addressed when deriving sets of spectrum-consistent ground motions: (a) referring to earthquakes that are representative of the seismogenic characteristics of the involved area; (b) obtaining the shortest possible accelerograms to reduce the computational burden of the analyses, particularly when they are non-linear ones. Both such issues are addressed in the present paper. Issue (a) is addressed by performing wide research in seismic databases to find earthquakes recorded in the Lebanese area, and proper elaborations of the selected records to obtain sets of spectrum-consistent accelerograms. Issue (b) is addressed by proposing a procedure that allows to suitably cut given spectrum-consistent earthquakes and obtain effective and energy-saving shorter accelerograms. Based on the Arias intensity, this procedure takes into consideration the intensity limits proposed by [21]. A reducing time step method was also proposed in [22], which extended a previously proposed method to non-linear systems [23]. The procedure

proposed in the present paper is an alternative viable method that is shown to be rather effective and easily performed with the help of commercial programs.

With reference to the two codes presently still in force (of the four referred to by the Lebanese code), suitable sets of full-length and short-length spectrum-consistent accelerograms are obtained and made available for the Lebanese design. A final investigation is provided to compare the results obtained by carrying out MRSAs, with reference to the different allowed DRS, and LTHAs under the short-length SCEs.

2. Seismicity of Lebanon

The tectonic complexity of the Eastern Mediterranean area is well known, see Figure 1a. Lebanon lies astride the Dead Sea Transform Fault (DSTF) in a region of complex tectonic plate interaction, where there are three major plates (the Arabian, African and Eurasian Plates) and two sub-plates (the Anatolian and Sinai subplates) [20]. The DSTF is a strike–slip fault between the African and the Arabian plates [24], which extends South–North approximately 1000 km from the north of the Gulf of Aqaba through Wadi Araba, the Dead Sea, the Jordan valley, the Beqaa valley, and merges eventually at the east of the Anatolian fault [25]. It can be divided into two main sections joined by a restraining bend along Lebanon, where it splits into five main fault branches: the Yammouneh, Roum, Serghaya, Rachaiya and Hasbaya faults, see Figure 1b. The activity of these faults has been the topic of recent paleoseismic [10,11] and geodetic [26] investigations which indicated that such faults are still active. Lebanon experienced many major earthquakes during its history. The 1759 one, that hit Beirut and Damascus may be considered the most destructive of the modern era. More recently, the 1956 earthquake was a destructive multiple-shock earthquake (5.3 and 5.5 Richter degrees) with its epicenter located in the Chouf District. A list of some of the strongest Lebanese earthquakes is provided in Table 1, as obtained from the literature [27–30].

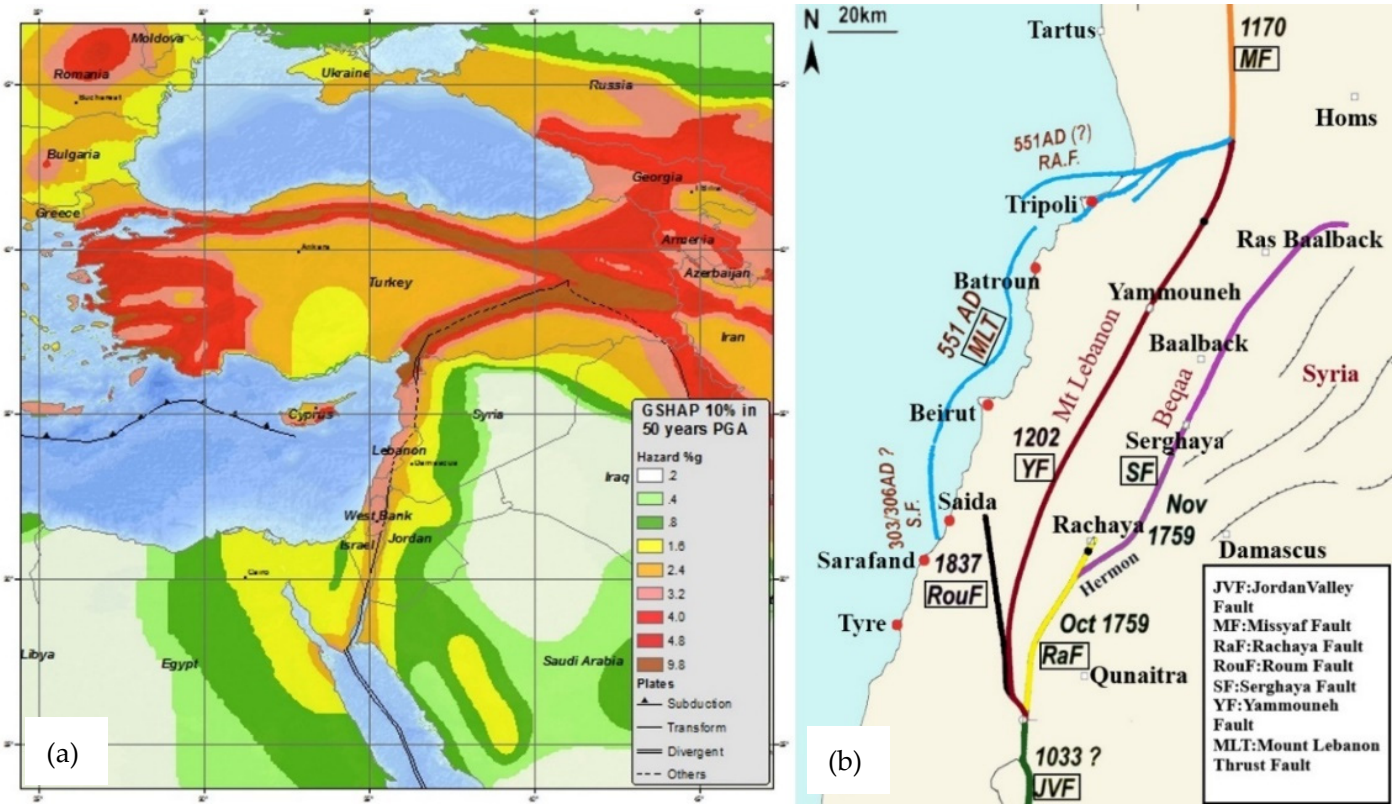

Figure 1. (**a**) Seismic map of the Eastern Mediterranean area; (**b**) active faults in Lebanon.

Table 1. Some of the strongest Lebanese earthquakes.

	Date	Location	Magnitude
1	9 July 551 A.D.	Phoenicia (Roman Province), Byzantine Empire (now Lebanon)	7.5
2	15 August 1157	Hama, West central Syria	>7.0
3	29 June 1170	Idlib, Northwestern Syria	>7.0
4	20 May 1202	Southwestern Syria	7.6
5	30 October 1759	Ottoman Syria part known today as Lebanon	6.7
6	25 November 1759	Ottoman Syria part known today as Lebanon	7.4
7	26 April 1796	Ladhikiya, Southwestern Syria	6.6
8	13 April 1822	Aafarine, Beqaa, Lebanon	7.4
9	3 April 1872	Amik golu, Beqaa, Lebanon	7.2
10	29 September 1918	Northwest of Tartus, Syria	6.6
11	16 March 1956	Southeast of Baabda, Mohafazat Mont-Liban, Lebanon	5.3
	16 March 1956	Southwest of Zahle, Mohafazat Béqaa, Lebanon	5.5
12	26 March 1997	Nabatîyé et Tahta, Mohafazat Nabatîyé, Lebanon	5.0
13	15 February 2008	Tyros, South Governorate, Lebanon	5.1

3. Design Response Spectra for Lebanon

The first Lebanese seismic design rules were introduced in the early 1990s. Governmental decrees N. 646, N. 14293, and N. 7964, issued in 2004, 2005 and 2012, respectively, provided the seismic design rules which are currently adopted in Lebanon. Based on such decrees, the Lebanese Standards Institution (LIBNOR) issued the Standard NL135 [31]. The latter assumes the same seismic hazard for the whole Lebanese territory, classifying it as a 2c seismic zone. NL135 also instructs the designer to refer to (i) the French Norm PS92 [32], (ii) the Uniform Building Code (UBC) [33] or (iii) the International Building Code (IBC) [34], while announcing the adoption of (iv) the Eurocode 8 (EC8) [35] as the only seismic code in Lebanon.

To sum up, three different seismic design lines are currently allowed by Lebanese NL135, while a fourth one is mentioned as the future unique reference code. It is worth noting that some of the codes referred to by Lebanese NL135 are obsolete in their countries. This is the case of PS92, which is not in force anymore in France, where presently EC8 is the reference code. On the other hand, IBC is a recent code which incorporates other previous USA codes, including UBC. The latter is, however, still widely used in some developing countries such as Lebanon.

To get a complete picture of the seismic design tools allowed in Lebanon, the DRS relevant to PS92, UBC, IBC are derived in the following Sections 3.1–3.3. In addition, the DRS obtained from EC8 are provided in Section 3.4. All the DRS meet the Lebanese NL135 and LIBNOR recommendations and have been built under the assumptions listed below.

Assumption 1. *Only the elastic design response spectra are considered.*

Assumption 2. *The reference peak ground acceleration (PGA) is taken as equal to* 2.5 m/s^2.

Assumption 3. *A period range* 0 *s–*4 *s will be considered here in the spectra.*

Assumption 4. *A damping ratio of 5% is considered.*

Assumption 5. *The vertical seismic action is neglected.*

It is worth noting that Assumption 1 and Assumption 2 are mandatory. The first one, in fact, derives from the final purpose of this study which is obtaining SCEs for transient dynamic analyses. The acceleration records must in fact be obtained by referring to the elastic (and not to the reduced). On the other hand, Assumption 2 meets the Lebanese code recommendations which assume a seismic zone factor Z = 0.25 and thus PGA $= 2.5$ m/s^2. Regarding Assumption 3, it should be noted that 0 s–4 s is the range where the fundamental

period of buildings typically falls, and in fact some codes, like the EC8 (see Section 3.4), confine the use of the design response spectra to this range. As far as Assumption 4 is concerned, it is noted that 5% is taken by most codes as a reference value for the damping ratio, this value being a realistic one for reinforced concrete and steel buildings. On the other hand, it is assumed this value would lead to conservative results for more dissipative materials such as masonry or timber. Finally, Assumption 5 is justified by the fact that the vertical component of the ground motion slightly affects buildings and, according to seismic codes, it should be accounted for only in particular cases (e.g., long-span bays, floor beams supporting columns, bridges). It is worth noting, however, that the vertical component of the earthquake might influence the post-elastic performance of some kinds of buildings [36].

It is worth noting that for the sake of a comprehensive study, the DRS obtained from PS92, UBC, IBC and EC8 will be derived in this section and compared in Section 4, according to the Lebanese NL135 code. In contrast, when deriving the SCEs and reducing them in Sections 5–7, reference only to IBC and EC8 will be given. The motivations of this choice are: (i) IBC is currently the reference code for the seismic design in USA, where UBC is not mandatory anymore; (ii) PS92 is an obsolete code in France, where EC8 is presently the reference code for the seismic design; (iii) EC8 is expected to be the only code which the Lebanese seismic design will be based on in the near future; (iv) almost all the Lebanese engineering schools refer to IBC and/or to EC8; (v) reference to IBC and EC8 is also typically used in the literature when dealing with Lebanese seismic design [19,20,37].

3.1. Design Response Spectra According to PS92

According to Annex A of PS92, the following formulas should be used to obtain the four branches of the normalized elastic design spectrum in terms of acceleration S_e as a function of the period T:

$$S_e(T) = A_n\,\tau\,[(R_A + (R_M - R_A)]\left(\frac{T}{T_B}\right) \text{ for } 0 < T \le T_B \quad (1)$$

$$S_e(T) = A_n\,\tau\,R_M \text{ for } T_B < T \le T_C \quad (2)$$

$$S_e(T) = A_n\,\tau\,R_M\,\left(\frac{T_C}{T}\right) \text{ for } T_C \le T \le T_D \quad (3)$$

$$S_e(T) = A_n\,\tau\,R_M\left(\frac{T_C}{T}\right)\left(\frac{T_D}{T}\right) \text{ for } T \ge T_D \quad (4)$$

Here A_n is the nominal peak ground acceleration (taken as equal to 2.5 m/s^2 according to Assumption 2), while τ denotes the topographic amplification factor, the values of which may range between 1 and 1.4, depending on the downstream and upstream slopes of the site, the greater the slope the higher the value of τ. Both the lowest and the highest values of τ are used here to obtain the DRS for the two extreme topographical conditions.

Four site types, namely S0, S1, S2 and S3, are considered by PS92, depending on the ground characteristics and on the depth of the soil layer above the bedrock. Three soil categories are classified by PS92, namely *a* (good or very good mechanical characteristics), *b* (medium mechanical characteristics) or *c* (low mechanical characteristics). Site S0 encompasses rock-like soils and/or layers of *a* soil not exceeding 15 m deep; site S1 includes more than 15 m deep *a* soil layers and/or less than 15 m deep *b* soil layers; site S2 includes soil *b* with depth between 15 m and 50 m and/or less than 10 m soil *c* layers; site S3 is characterized by more than 50 m deep layers of b soil and/or layers of *c* soil with depth between 10 m and 100 m. The reader may refer to PS92 for a more detailed description of the different site and soil types.

The horizontal normalized elastic DRS relevant to the four site types and to $\tau = 1$ and $\tau = 1.4$ are provided in Figures 2a and 2b, respectively. The spectra are obtained by

assuming the values given in Table 2 for the characteristic periods T_B T_C and T_D and for the parameters R_A and R_M, all these values being in accordance with the Lebanese code indications. It can be noted that on the third branch of the spectra the accelerations (and thus the design forces) are higher for softer soils, which is due to the well-known soft soil amplification effect.

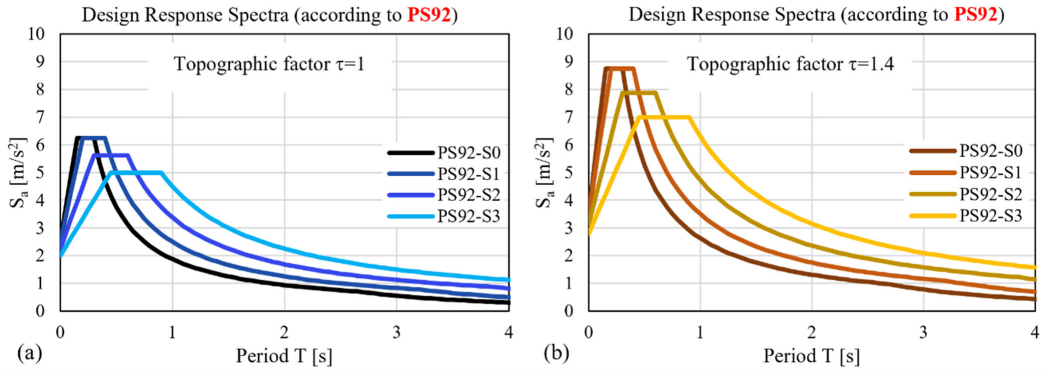

Figure 2. Lebanese horizontal design response spectra as obtained according to PS92 for the four site types (S0, S1, S2, S3) and 5% damping. (**a**) Spectra for $\tau = 1$; (**b**) Spectra for τ =1.4.

Table 2. Values of the parameters according to Table A.1 of Annex A of PS92 [32].

Soil Type	T_B	T_C	T_D	R_A	R_M
S0	0.15	0.30	2.67	1.00	2.50
S1	0.20	0.40	3.20	1.00	2.50
S2	0.30	0.60	3.85	0.90	2.25
S3	0.45	0.90	4.44	0.80	2.00

3.2. Design Response Spectra According to UBC

When reference to the Uniform Building Code (UBC) is made, the DRS can be obtained through the following formulas giving the horizontal absolute acceleration S_e as a function of the period T:

$$S_e(T) = \left(\frac{1.5 * C_a}{T_0}\right) * \mathrm{T} + C_a \text{ for } T \leq T_o \tag{5}$$

$$S_e(T) = 2.5 * C_a \text{ for } T_o < T \leq T_s \tag{6}$$

$$S_e(T) = \frac{C_v}{T} \text{ for } T \geq T_s \tag{7}$$

Here T_o and T_s are the characteristic periods at the end and start of the different spectrum branches. They are defined as:

$$T_0 = 0.2 * T_s \tag{8}$$

$$T_s = \frac{C_v}{2.5 C_a} \tag{9}$$

The coefficients C_a and C_v depend on the soil conditions at the site and on the seismicity of the region. Their values are provided in Table 3 as obtained according to NL135 for the five site classes considered by UBC, namely, A, B, C, D and E. The site classes are characterized by the kind of soil and the average shear wave velocity at 30 m depth (V_{s30}). Table 4 collects the main characteristics defining the different site classes. The reader may refer to UBC for further details about the characteristics of site classes. The resulting five

spectra are displayed in Figure 3a. In addition to Equations (5)–(7), a further formula is also given by UBC which defines a branch of the spectra for values of period exceeding 4 s. According to Assumption 3 of Section 3, this branch is not considered in this study.

Table 3. Values of the parameters for different site classes (according to UBC, IBC and NL135).

Site Class	UBC		IBC			
	C_a	C_v	S_1	S_s	F_a	F_v
A	0.20	0.20	0.4	1.2	0.8	0.8
B	0.25	0.25	0.4	1.2	1.0	1.0
C	0.29	0.40	0.4	1.2	1.0	1.4
D	0.32	0.47	0.4	1.2	1.0	1.6
E	0.35	0.74	0.4	1.2	0.9	2.4

Table 4. Site classes according to UBC and IBC.

Site Class	Average Properties at 30 m Depth		
	Shear Wave Velocity	Standard Penetration Resistance	Undrained Shear Strength
	$v_{s,30}$ (m/s)	N_{SPT} (blows/30 cm)	S_u (kPa)
A	>1500	-	-
B	760–1500	-	-
C	360–760	>50	>100
D	180–360	15–50	50–100
E	<180	<15	<50

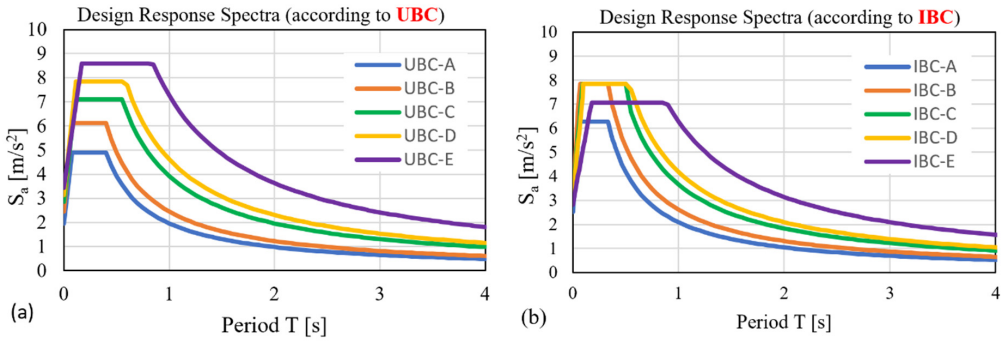

Figure 3. Lebanese horizontal design response spectra as obtained according to American (**a**) UBC and (**b**) IBC codes for the five soil types (A, B, C, D, E) and 5% damping ratio.

3.3. Design Response Spectra According to IBC

The *International Building Code* (IBC) gives the following formulas to build the DRS in terms of horizontal absolute acceleration $S_e(T)$:

$$S_e(T) = S_{DS} * \left[0.4 + 0.6 * \left(\frac{T}{T_0}\right)\right] \text{ for } T \leq T_o \tag{10}$$

$$S_e(T) = S_{DS} \text{ for } T_o < T \leq T_s \tag{11}$$

$$S_e(T) = S_{D1}/T \text{ for } T \geq T_s \tag{12}$$

IBC also gives a fourth branch of the spectrum that applies for values of period exceeding 4 s, similarly to UBC. This branch will not be considered here, according to Assumption 3. The values of S_{DS}, S_{D1} T_0 and T_s can be obtained through the formulas:

$$S_{DS} = \frac{2}{3} * S_{MS} \tag{13}$$

$$S_{MS} = F_a * S_s \tag{14}$$

$$S_{D1} = \frac{2}{3} * S_{M1} \tag{15}$$

$$S_{M1} = F_v * S_1 \tag{16}$$

$$T_0 = 0.2\frac{S_{D1}}{S_{Ds}} \tag{17}$$

$$T_s = \frac{S_{D1}}{S_{Ds}} \tag{18}$$

The values of the parameters S_1, S_s, F_a and F_v are provided in Table 3, in accordance with NL135, for the five site classes defined in Table 4 (the same classes are referred in fact by IBC and UBC). The DRS obtained through Equations (10)–(18) and Table 3 are displayed in Figure 3b, which are the same for the two main horizontal directions. It is noted that on the third branch of the IBC spectra the design acceleration increases as the mechanical properties of the soil decrease (as PS92). The UBC spectra follow the soft soil amplification rule all over the period range instead. When comparing Figure 3a,b, it can be inferred that, for the Lebanese design, UBC is almost always less conservative than IBC (site classes A, B and C), or similarly conservative (site class D).

3.4. Design Response Spectra According to Eurocode 8

The NL135 standard announced the transition to Eurocode 8 as the exclusive seismic code applicable in Lebanon within the next five years. In view of this, French Universities instruct on EC8, and engineers incorporate it into their designs of buildings by adopting parameters identical to those assumed for PS92.

The DRS in terms of horizontal absolute acceleration $S_e(T)$ are given by EC8 as follows:

$$S_e(T) = a_g\ S\left[1 + \frac{T}{T_B}(2.5\eta - 1)\right] \textit{for}\ 0 < T \leq T_B \tag{19}$$

$$S_e(T) = 2.5\ a_g\ S\ \eta \text{ for } T_B < T \leq T_C \tag{20}$$

$$S_e(T) = 2.5\ a_g\ S\ \eta\left[\frac{T_C}{T}\right] \text{ for } T_C \leq T \leq T_D \tag{21}$$

$$S_e(T) = 2.5\ a_g\ S\ \eta\left[\frac{T_C T_D}{T^2}\right] \text{ for } T_D \leq T \leq 4\text{ s} \tag{22}$$

Here a_g is the reference peak ground acceleration, taken equal to 2.5 m/s^2 according to Assumption 3, while η is a damping correction factor given by

$$\eta = \sqrt{10/(5+\xi)}\ \geq 0.55 \tag{23}$$

ξ being the damping ratio taken equal to 5% according to Assumption 4. The EC8 Type 1 shape for the elastic response spectrum is chosen. The use of two alternative shapes of DRS (Type 1 or Type 2) is in fact allowed by EC8. When the seismic hazard of the most contributing earthquake for the considered site has a surface-wave magnitude not greater than 5.5, Type 2 is recommended, otherwise Type 1 should be better used. Since the magnitude of Lebanese earthquakes may even greatly exceed 5.5, as can be inferred from Table 1, the Type 1 shape is here assumed for the elastic DRS, this choice being on the safe side. Five ground types are considered by EC8, as recalled by Table 5. The values of the

soil factor S and of the periods T_B, T_C and T_D for the Type 1 shape and for the five ground types are recalled in Table 6. The EC8 design spectra obtained for the five ground types and relevant to both the horizontal components are plotted in Figure 4. Similarly, to PS92 and IBC, EC8 follows the soft soil amplification rule in the third branch of the spectra.

Table 5. Ground types according to EC8.

Ground Type	Average Properties at 30 m Depth		
	Shear Wave Velocity	Standard Penetration Resistance	Undrained Shear Strength
	$v_{s,30}$ (m/s)	N_{SPT} (Blows/30 cm)	c_u (kPa)
A	>800	-	-
B	360–800	>50	>250
C	180–360	15–50	70–250
D	<180	<15	<70
E	Soil profile consisting of a surface alluvium layer with v_s values of type C or D and thickness varying between 5 m and 20 m, underlayed by stiffer material with $v_{s,30} > 800$ m/s		

Table 6. Values of the parameters for the Type 1 response spectrum (according to EC8).

Ground Type	S	TB (s)	TC (s)	TD (s)
A	1.00	0.15	0.4	2.0
B	1.20	0.15	0.5	2.0
C	1.15	0.20	0.6	2.0
D	1.35	0.20	0.8	2.0
E	1.40	0.15	0.5	2.0

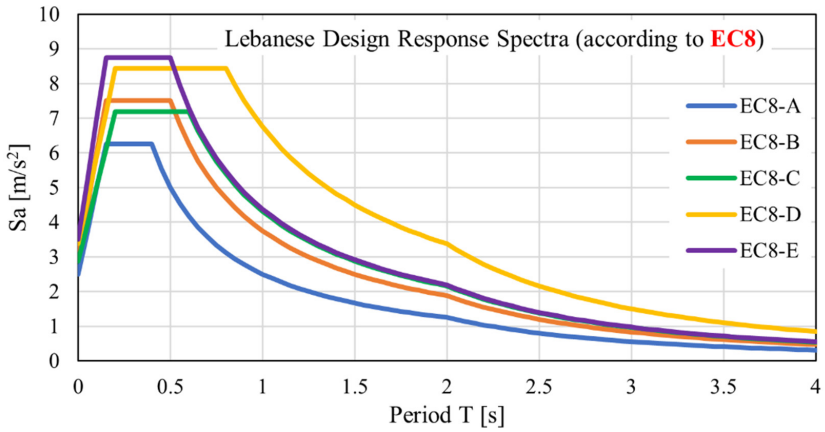

Figure 4. Lebanese horizontal design response spectra as obtained according to EC8 for the five soil types (A, B, C, D, E) and 5% damping ratio.

4. Comparing Lebanese Design Response Spectra

In the present section the DRS to which NL135 refers are compared in order to check the different safety levels allowed by the Lebanese design rules. For this purpose, the four main categories listed in Table 7 were assumed as giving a good correspondence between the site/ground classifications made by PS92, UBC, IBC and EC8. It is worth noting that a clear equivalence can be held between the EC8 and the UBC/IBC classification [30], while a straightforward correlation cannot be easily assigned between PS92 and the other codes. Both EC8 and IBC classify sites based on the average shear wave velocity, denoted as $v_{s,30}$, calculated within the uppermost 30 m of the soil strata. In contrast, the French PS92 employs diverse depth criteria for its site classification. To ensure a suitable comparative analysis, a standardized depth of 30 m was here considered, facilitating the harmonization of site/ground classifications of IBC and EC8 with that of PS92. This led to deriving the four primary categories outlined in Table 7. A representation of the DRS for each of these categories, along with two specified values of the PS92 topographical factor τ, is presented

in Figure 5. The diagrams on the left (Figure 5a,c,e,g) refer to $\tau = 1$ and those on the right (Figure 5b,d,f,h) to $\tau = 1.4$.

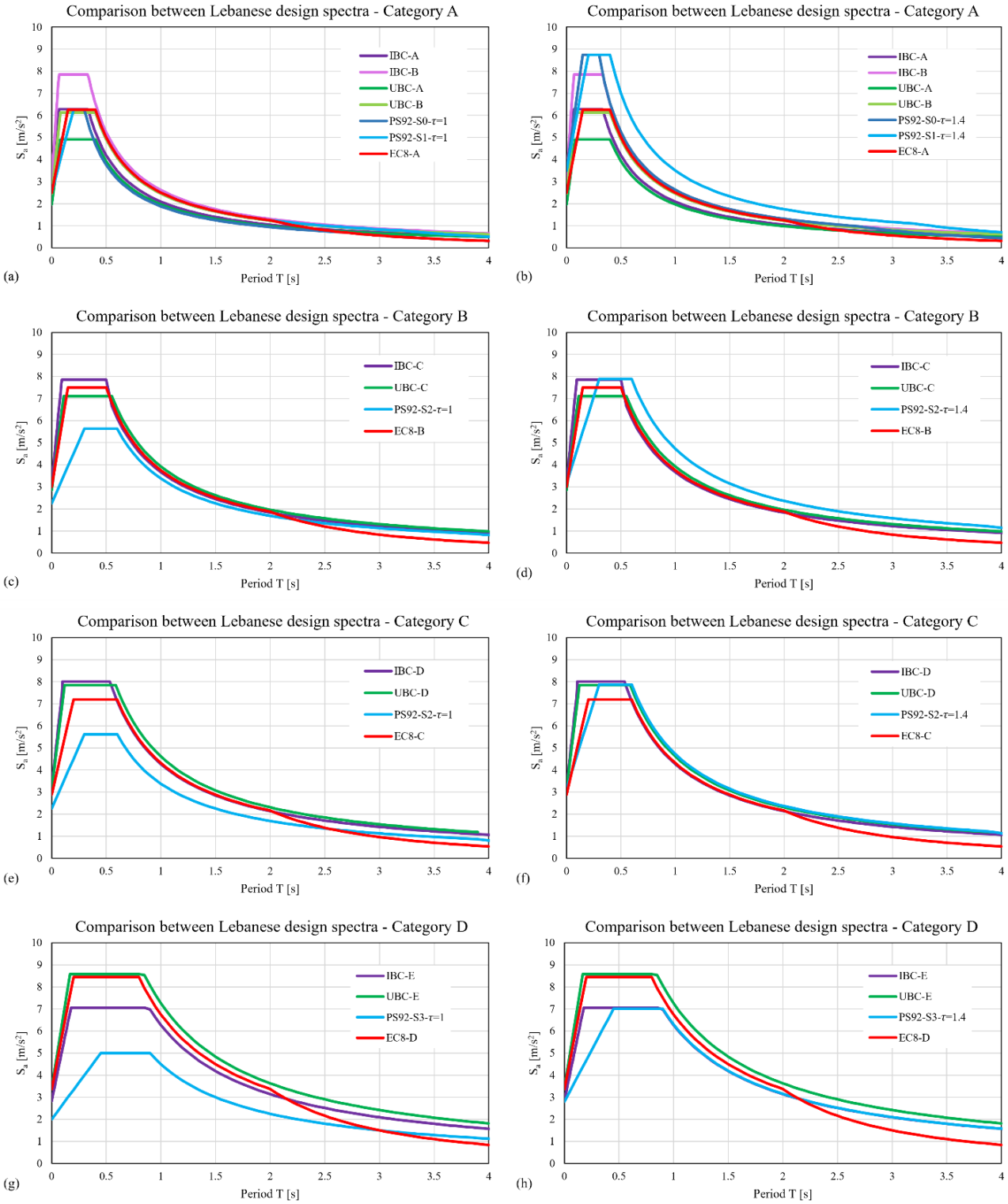

Figure 5. Comparison between the design spectra given by the considered codes for different soil types: (**a**) Category A with τ = 1 for spectra of PS92, (**b**) Category A with τ = 1.4 for spectra of PS92, (**c**) Category B with τ = 1 for spectra of PS92, (**d**) Category B with τ = 1.4 for spectra of PS92, (**e**) Category C with τ = 1 for spectra of PS92, (**f**) Category C with τ = 1.4 for spectra of PS92, (**g**) Category D with τ = 1 for spectra of PS92, (**h**) Category D with τ = 1.4 for spectra of PS92.

Table 7. Correspondence table for the different site/ground categories.

Category	Site/Ground Class/Type		
	PS92	UBC/IBC	EC8
A	S0	A	A
	S1	B	
B	S2	C	B
C		D	C
D	S3	E	D

The comparisons provided in Figure 5 show that different design seismic forces can be considered for structures with similar dynamic properties (fundamental period T) and for the same site/ground type. This may lead to different safety levels in the Lebanese design.

5. Suites of Earthquakes Consistent with the Lebanese DRS

Suitable earthquakes are needed to carry out time-history analyses for the seismic design/assessment of new/existing buildings. Codes give instructions on how to obtain accelerograms consistent with the reference design spectrum, which is related to the seismicity of the site. Artificial or real records can be used for this purpose. In the present work, reference to real records was made to obtain some suites of spectrum-consistent accelerograms for the Lebanese seismic design. The suites are obtained referring only to the IBC and the EC8 elastic design response spectra, according to the motivations given in Section 3. The motivations of this choice are: (i) IBC is currently the reference code for the seismic design in USA, where UBC is not mandatory anymore; (ii) PS92 is an obsolete code in France, where EC8 is presently the reference code for the seismic design; (iii) EC8 is expected to be the only code which the Lebanese seismic design will be based on in the near future.

The procedure to obtain the spectrum-consistent accelerograms consists of the following three main steps.

5.1. Step 1. Collecting Suitable Records

Preliminary research of suitable records was made by exploring ESM [38] and COSMOS [39] databases and confining the attention to earthquakes that occurred in the Lebanese area. Since very few records are found for Lebanon, the research was extended to a wider area of the Middle East region, also including the Dead Sea, the Mediterranean Sea, Syria, and Turkey. Among the several earthquakes retrieved, thirteen have been finally selected as suitable enough for the purpose. The criteria for this choice mainly involved identifying a significant number of recorded strong ground motions that occurred along the DSTF, which is the strike–slip fault zone where Lebanon lies. This was assumed to guarantee the chosen earthquakes have similar characteristics, belonging to the same seismogenic source. Table 8 lists the selected earthquakes, which are here labelled from E1 to E13. Each earthquake is decomposed into a couple of records giving the acceleration in the two main horizontal directions (the vertical component is neglected according to Assumption 5 of Section 3). Such a collection of earthquakes will be exploited to obtain suites of appropriate synthetic accelerograms. It can be noted that some of the earthquakes listed in Table 8 have a low magnitude value. In consideration of the scarcity of records, however, such lower-magnitude earthquakes have been considered. This is not a limit since the elaboration process described in Step 2 leads, in any case, to spectrum-matched final synthetic records. The matching process, in fact, is based on code DRS that account for the actual seismicity of Lebanon and the expected peak ground acceleration level. Thus, the final accelerograms that are eventually obtained through the synthetization procedure are stronger than the original ones and typically correspond to earthquakes with more than 5.5 magnitude. Suitably matching the original earthquakes is advised when there is a lack of instrumental records.

Table 8. Suite of earthquakes chosen to obtain the accelerograms consistent with the design spectra.

Id.	Station Code	Event ID	Location	Date	Magnitude
E1	UJAP	EMSC-20140524_0000020	Dead Sea	24 May 2014	4.3 (M_L)
E2	GHAJ	EMSC-20180704_0000036	Dead Sea	7 April 2018	4.1 (M_W)
E3	MSBI UJAP	EMSC-20180704_0000512	Dead Sea	7 April 2018	4.7 (M_W)
E4	GHAJ MSBI	EMSC-20190626_0000058	Dead Sea	26 June 2019	4.0 (M_W)
E5	IZR	IL-1984-0002	Dead Sea	24 August 1984	5.3 (M_W)
E6	KRKR SUAN	SY-1996-0001	Jordan–Syria	24 December 1996	5.5 (M_W)
E7	3101 3103	TK-2006-0033	Jordan–Syria	29 March 2006	4.1 (M_W)
E8	EIL	EMSC-20110220_0000203	Red Sea	20 February 2011	3.7 (M_L)
E9	CMRD SLFK	EMSC-20200415_0000051	Syrian Coast	15 April 2020	4.7 (m_b)
E10	KRTS	EMSC-20200403_0000177	Syrian Coast	3 April 2020	4.7 (M_W)
E11	KRTD	EMSC-20130726_0000002	Central Turkey	26 July 2013	4.3 (M_W)
E12	BOZY KRTD	EMSC-20120511_0000032	Cyprus Rgion	11 May 2012	5.3 (M_W)
E13	OSC1 OSC2	EMSC-20170108_0000026	Cyprus Rgion	8 January 2017	4.1 (M_L)

5.2. Step 2. Obtaining Suites of Spectrum-Consistent Earthquakes

Codes recommend using a suite of SCEs when carrying out time-history analyses. A minimum number of three earthquakes is suggested by EC8 as well as by ASCE 7-16 [40], to which IBC refers on this matter. Should a suite of seven earthquakes be considered, both codes allow the averaging of the results from the seven analyses. Different methods can be used to find the most appropriate set of ground motions, ranging from just a selection of real records based on their seismological characteristics to more powerful matching procedures that are carried out in the frequency domain through wavelet adjustments over one or multiple target spectra [41]. The number of records required to obtain a stable and unbiased estimate of the inelastic response of a structure was found to significantly depend on the method adopted [42]. When simpler methods like those that scale the accelerograms to the target spectral acceleration are applied, a higher number of accelerograms is needed. This number can be reduced when the Spectral Matching (SM) method is applied instead. The scarcity of recorded ground motions in a country may thus be a reason to adopt the SM method [43]. The SM changes both the amplitude and the frequency content of the earthquake to make its response spectrum match the target design one, this procedure generally leading to more stable results [42]. The addition of wavelets has the same advantages provided by the Fourier adjustment with the extra benefit of introducing less energy into the ground motion and preserving the non-stationary characteristics of the original ground motion [41]. Based on previous studies [44–46], an effective SM algorithm was developed by Abrahamson [47], and subsequently refined by Hancock et al. [41].

Due to the rarity of strong recorded earthquakes in the Lebanese area and to the higher effectiveness of the SM method with respect to other methods, the latter is adopted in the present study. Based on the Abrahamson–Hancock algorithm, the SeismoMatch [48] application is used to obtain suites of earthquakes consistent with the IBC design spectra (Figure 3b) and with the EC8 design spectra (Figure 4). For this purpose, the values of the matching parameters listed in Table 9 and the earthquakes listed in Table 8 were considered in SeismoMatch. In Table 9, the mismatch tolerance denotes the maximum allowable discrepancy between the matched earthquake spectrum and the target one. It is noted that SeismoMatch allows setting one single value for the mismatch tolerance, which means giving the same value to the upper and lower bounds. EC8 suggests a 10% lower bound, but it does not give an upper bound. On the other hand, IBC does not provide specific

values for mismatch tolerance. The matter of ground motion selection and modification for new building projects in the United States was recently addressed by the Building Seismic Safety Council in FEMA P-1050 [49] as also discussed in [50]. Although a 10% lower bound is suggested by BSSC for scaled earthquakes, no specific values are given instead for matched earthquakes, the spectra of which are only required not to fall below the target spectrum. It is also worth noting that some codes provide a lower and an upper tolerance bound such as the Italian Code [51] that provides a 10% and a 30% lower and upper tolerance limit, respectively. The absence of a prescribed upper tolerance bound may have an impact on the seismic design, since it allows the designer to refer to sets of spectrum-consistent earthquakes that may have very different violence levels, although matching the same target spectrum; this matter was discussed for instance in [9] with reference to EC8.

Table 9. Values of the matching parameters used in SeismoMatch.

Mismatch Tolerance	Max Iterations	Scale Factor	Min Eigenvalue	Max Number of Waves	Additional Waves	Off Diagonal Reduction	Group Size
0.1	200	1	0.1	10	20	0.7	250

In this study, 10% upper and lower bounds were adopted (mismatch tolerance equal to 0.1). This choice is also in accordance with what was assumed in other studies [50]. The number of maximum iterations was set to 200 for a scale factor of 1. The default value was adopted for the other parameters appearing in Table 9, which are related to the Abrahamson–Hancock algorithm [26]. Typically, the higher the maximum number of waves for the wavelet model, the better the matching outcome, although considering more than ten waves have no significant effect on the results. On the other hand, 20 additional waves (or sub-iterations) are enough to prevent divergence in the Abrahamson–Hancock algorithm, as shown in [42]. Better convergence can even be reached when the off-diagonal terms of the response-to-time matrix do not exceed the 0.7 value recommended by SeismoMatch, and the design spectrum is split into sub-groups, the recommended number of which is 250 [42]. Suites of SCEs were finally found according to IBC and EC8. They are presented in Sections 5.1 and 5.2, respectively.

5.3. Step 3. Deriving Suites of Shorth-Length Accelerograms for the Numerical Analyses

The suites of SCEs derived through the synthetization procedure described in Step 2 are generally long-time records (see for instance those provided in Sections 6 and 7). Therefore, reducing the time-length of the SCEs can be very useful. A method to achieve such a goal is proposed in Section 7, where the short-length IBC-consistent and EC8-consistent earthquakes are eventually determined.

6. Earthquakes Consistent with the IBC and the EC8 Design Spectra

By following the two-step procedure illustrated above, five suites of earthquakes consistent with the IBC design response spectra (see Figure 3b) and five other suites of earthquakes consistent with the EC8 design spectra (see Figure 4) were derived. It is noted that all the obtained accelerograms are baseline corrected. Figure 6 shows the spectra of the IBC-spectrum-consistent earthquakes in the two main directions compared with the target design spectrum for each of the five site classes. Figure 7 displays the accelerograms of the matched earthquakes. Similarly, the spectra and the accelerograms of the earthquakes consistent with the EC8 design spectra are provided in Figures 8 and 9 for the two main directions. It is worth noting that the matching procedure was carried out by considering the range 0–4 s according to Assumption 3 of Section 3. However, for a better comparison in the highest acceleration range, a shorter range (from zero to 2 s) was considered in the diagrams of Figures 6 and 8.

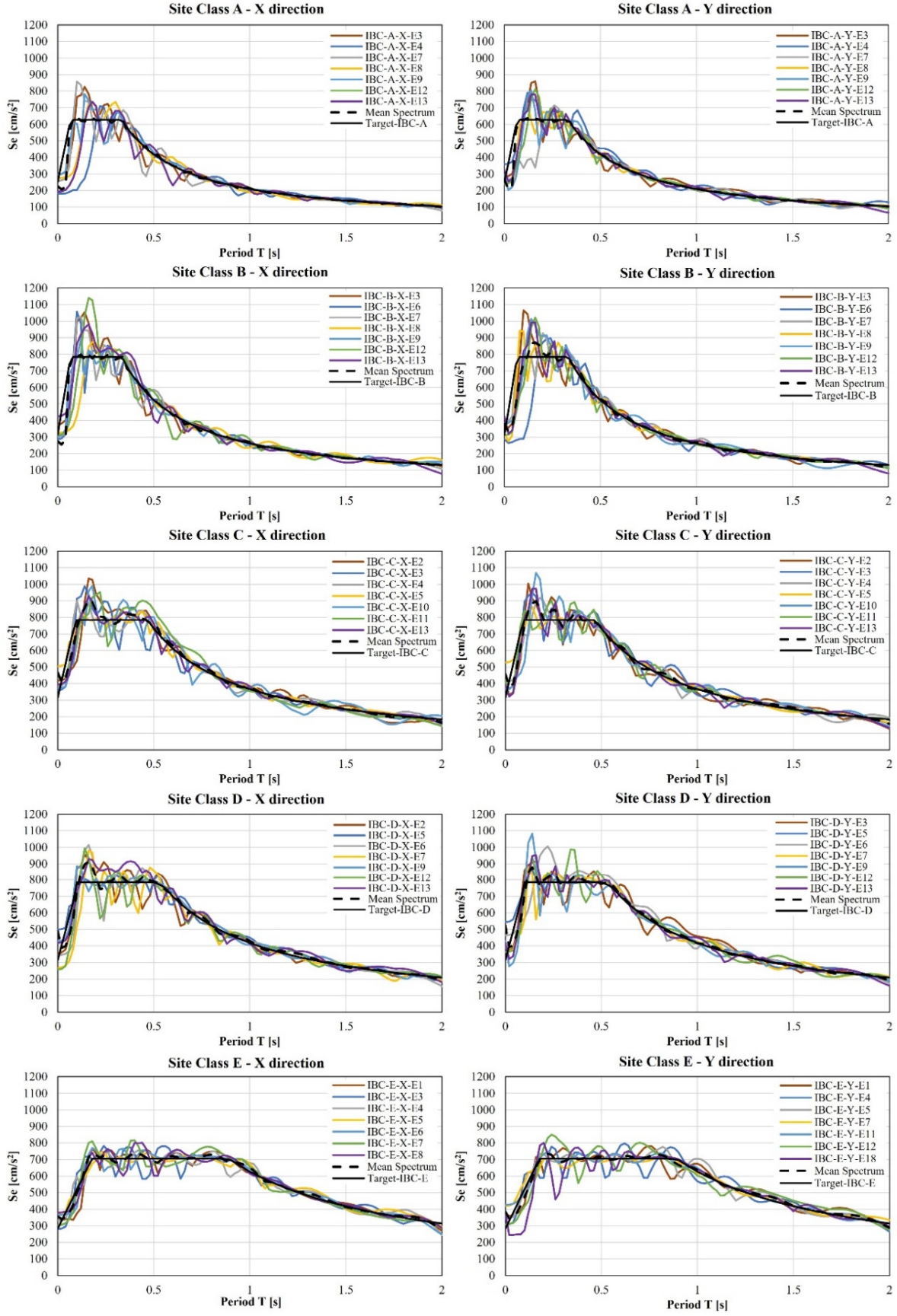

Figure 6. Target design spectra and response spectra of the suites of IBC-spectrum-consistent earthquakes in the *X* and *Y* direction (left and right diagrams) for the five soil types.

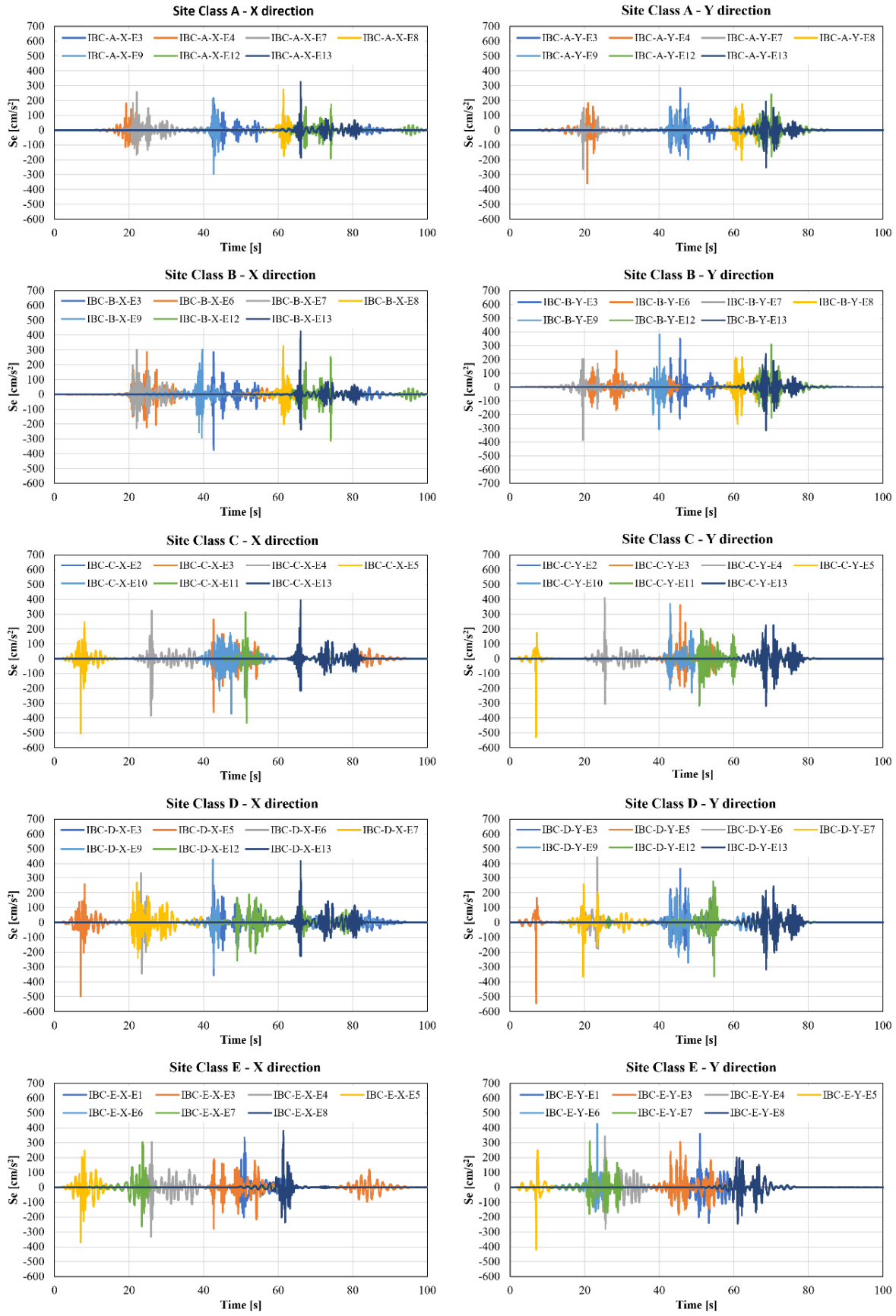

Figure 7. Accelerograms of the suites of IBC-spectrum-consistent earthquakes referred to in Figure 6.

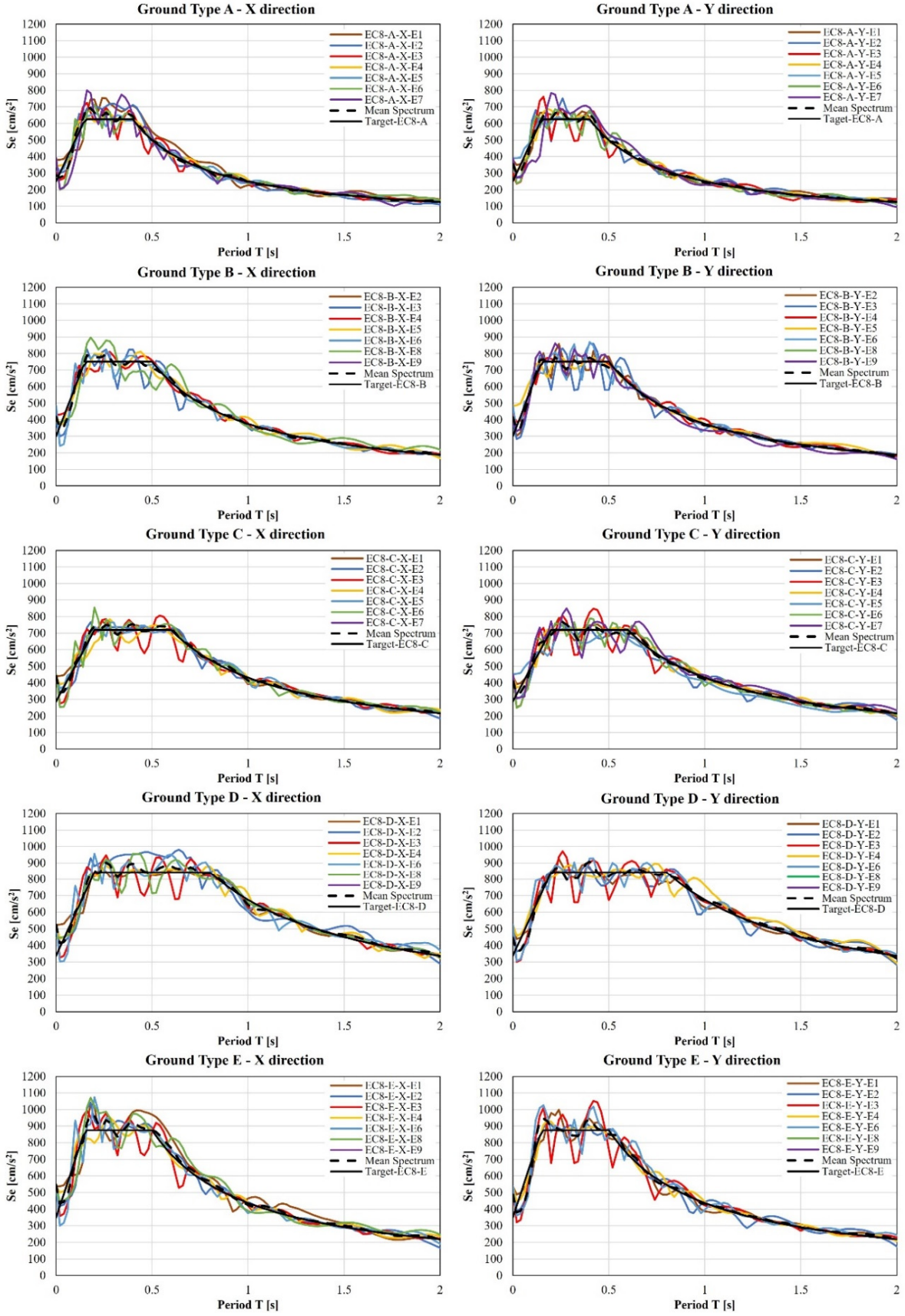

Figure 8. Target design spectra and response spectra of the five suites of EC8-spectrum-consistent earthquakes in the *X* and *Y* direction (left and right diagrams) for the five soil types.

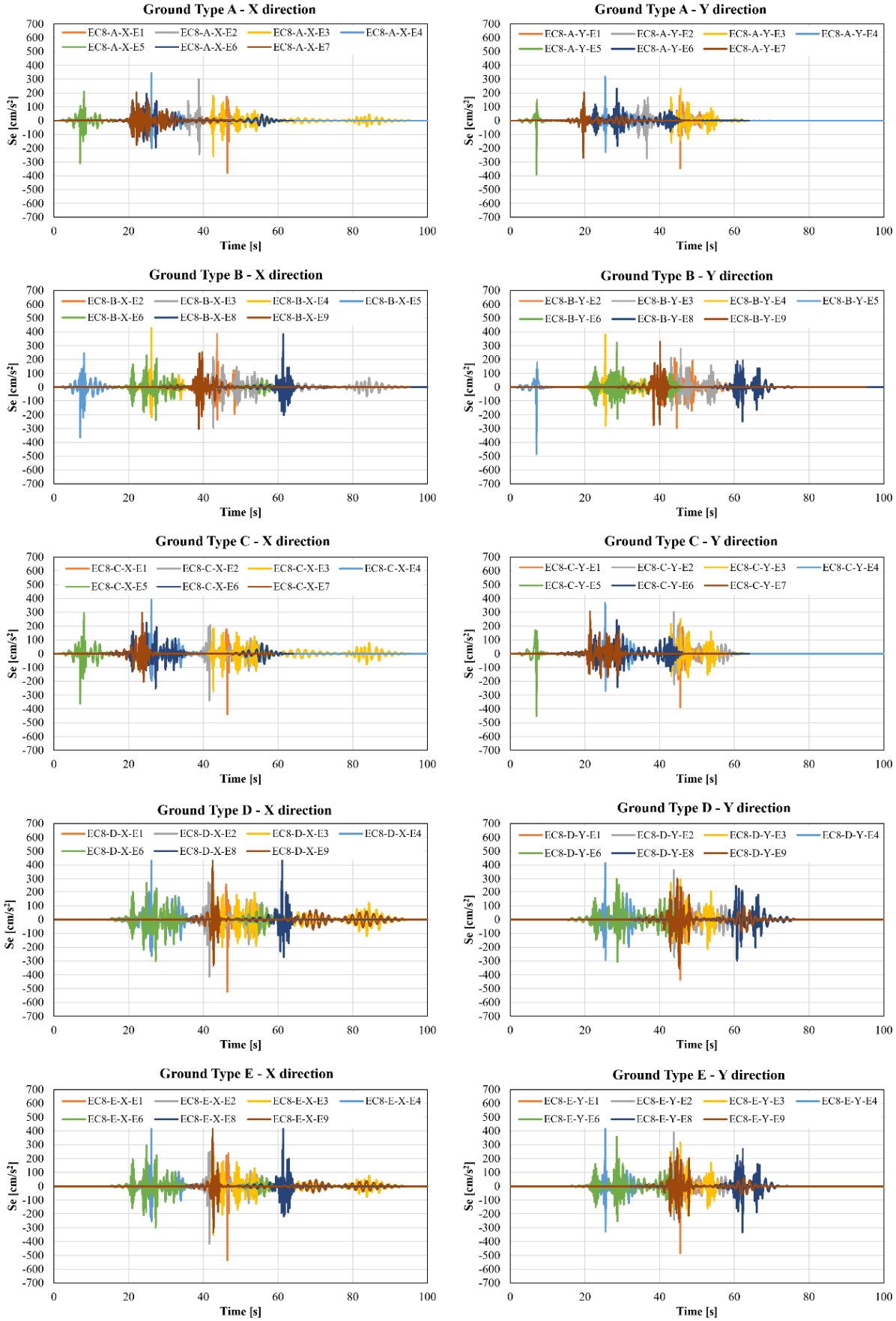

Figure 9. Accelerograms of the suites of EC8-spectrum-consistent earthquakes referred to in Figure 8.

Labelled as they are in Figures 6–9, the accelerograms are freely downloadable from a repository that is hosting them, as indicated at the end of the paper. They can be used for time-history (linear or non-linear) analyses of Lebanese structures. As derived from SeismoMatch, the records have a rather long time-length. A procedure to suitably reduce the time-length of spectrum-consistent accelerograms is proposed in Section 6.

7. Short-Length Energy-Saving Accelerograms for Numerical Analyses

Since NLTHAs generally involve a high computational demand, the ground motions introduced in the numerical model should be as short as possible. On the other hand, when cutting the full recorded accelerogram, the most significant peaks should be maintained and a high enough percentage of the seismic energy of the whole event conserved. To this end, the Arias Intensity I_A can be exploited. The Arias intensity was introduced as an indicator of the destructive potential of an earthquake, under the assumption that the damage experienced by a structure is proportional to the energy dissipated during the seismic event. It is defined as the integral of the dissipated energy $E(\omega)$ over the frequency domain [52]:

$$I_A = \int_0^{\omega} E(\omega)\, d\omega \tag{24}$$

In the time domain, I_A was expressed instead as the integral of the square acceleration over the complete duration t of the earthquake [45]:

$$I_A = \frac{\pi}{2g} \int_0^{t_d} a^2(t)\, dt \tag{25}$$

Here $a(t)$ is the ground acceleration, g is the gravity acceleration and t_d is the total duration of the record. The Arias intensity defined by Equation (25) is like the formulation used by Trifunac and Brady [21] when introducing the limits of the significant duration of an earthquake.

The Arias intensity can be exploited to find the most efficient and energy-conserving time-window of the earthquake. For this purpose, the SeismoSignal [53] program can be used. For any given filtered and baseline corrected ground motion, this program provides the effective duration of the earthquake corresponding to values of I_A from 5% to 95%. In the following, an example is given to illustrate how SeismoSignal can lead to obtaining a suitable time-window of a given earthquake.

Let us refer to the two components of one of the IBC-spectrum-consistent earthquakes displayed in Figure 7, namely IBC-C-X-E5 and IBC-C-Y-E5. Once the accelerograms (see Figure 10a) are uploaded in SeismoSignal and the option "effective duration" is set, the values given in Table 10 can be extracted. The diagrams in Figure 10b can also be extracted, where the time-windows relevant to the 5–95% range of I_A are highlighted in green. It should be noted that the starting and the final values of the time-windows are different for the two components, as can be inferred from Figure 10c. Since same-duration components of the earthquake must be given for the analyses, a single time-window should be set. An effective and energy-saving time-window could be defined by choosing the lowest time value and the highest time value of the two time-windows found through the Arias intensity procedure, see Figure 10d. Eventually the full-length accelerograms of Figure 10a are reduced to those shown in Figure 10e which are saving 95% of the earthquake energy, while being shortened to about $\frac{1}{4}$ of the full length. It is noted, in fact, that saving almost all the energy of the original ground motion is of paramount importance since the effects of ground motions on structures are strongly related to the energy input [54].

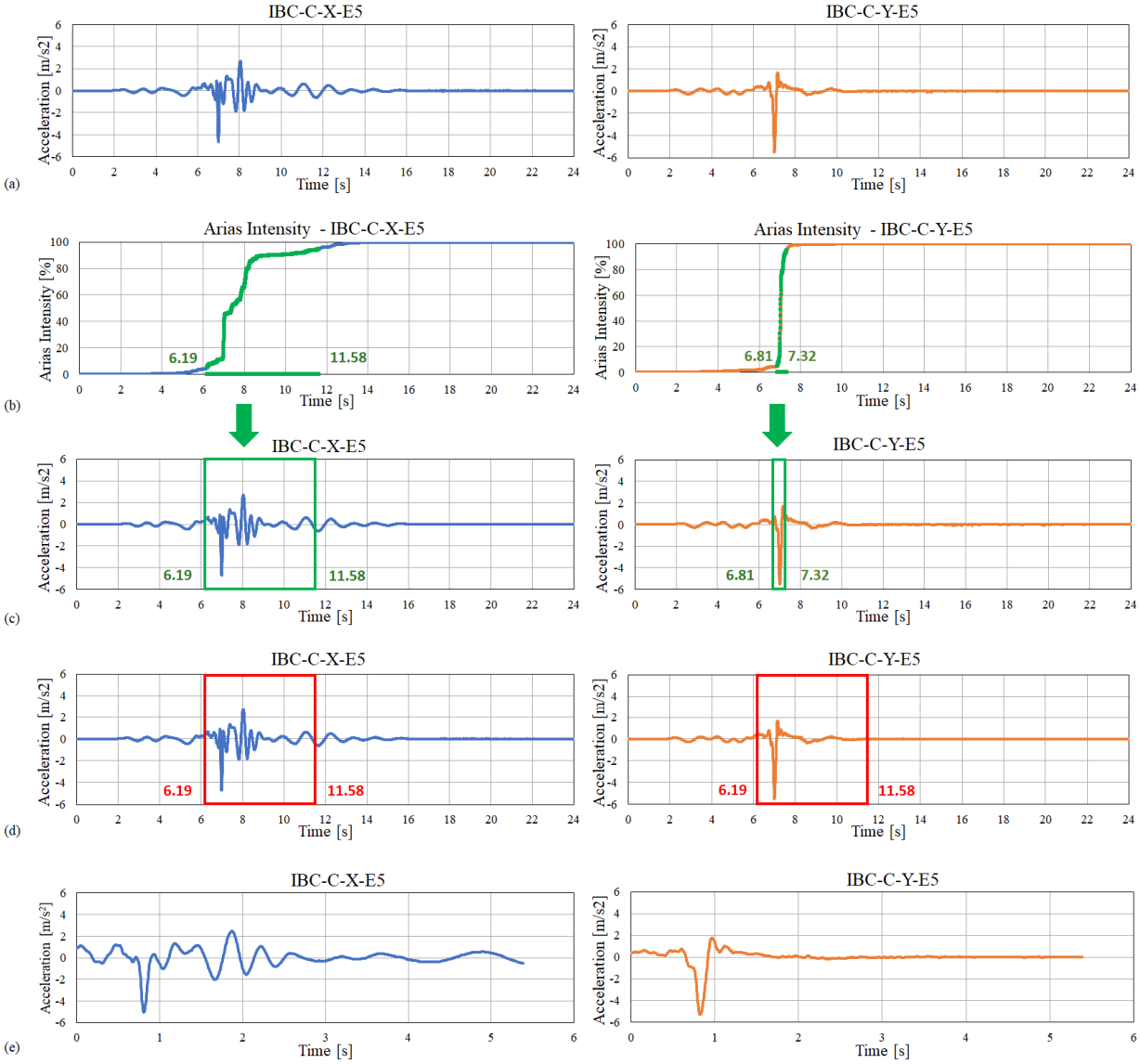

Figure 10. Procedure to obtain a suitable time-window for time-history analyses. (**a**) Full-length X and Y accelerograms; (**b**) Arias Intensity of the two components of the earthquake, where the range from 5% to 95% is highlighted in green; (**c**) time windows corresponding to 5–95% of I_A in green; (**d**) final chosen time-window for the two components, in red; (**e**) cut earthquake components for the numerical analyses.

Table 10. Duration and Arias Intensity for IBC-C-X-E5 (from SeismoSignal).

Earthquake Component	Duration [s]	Cumulative I_A [m/s]	Percentage of I_A [%]
IBC-C-X-E5	6.19	0.3	5
	11.58	6.2	95
IBC-C-Y-E5	6.81	0.2	5
	7.32	4.1	95

To validate the procedure, the planar four-story building displayed in Figure 11 was adopted as a simple archetype. The structural elements are made of reinforced concrete, with square columns measuring 50 cm on each side, and beams with a height of 50 cm and a base of 30 cm. Since the purpose of this validation is not to assess the design of the elements, symmetrical longitudinal reinforcement has been assumed for the columns, consisting of 12 bars of 20 mm and transverse bars of 10 mm spaced evenly every 10 cm.

Additionally, the beams have symmetrical longitudinal reinforcements for the upper and lower layers, consisting of 4 bars of 20 mm.

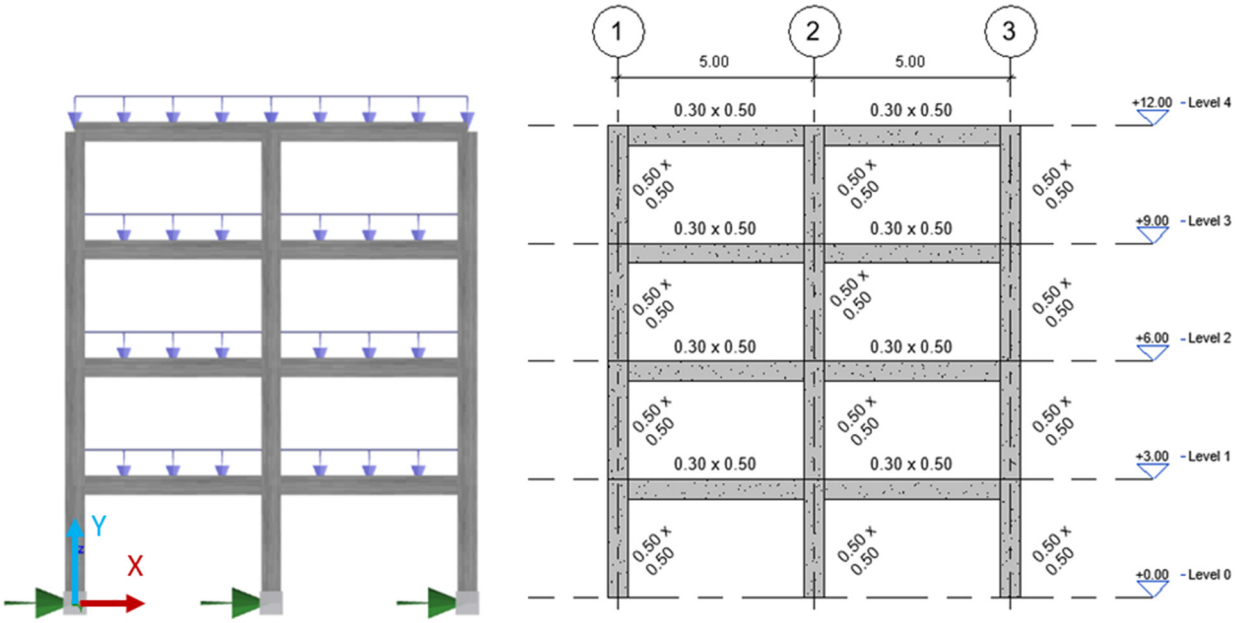

Figure 11. Elevation view of the structural archetype considered to validate the procedure.

The applied loads correspond to those of a building with solid reinforced concrete slabs measuring 15 cm in thickness, with a tributary width of the slabs of 3 m. The applied live loads correspond to those of a residential building (2 kPa). The archetype with gravity loads and the accelerations imposed on the supports in the *X* direction is shown in Figure 11.

NLTHAs were conducted by assuming that the reinforcing steel and the concrete follow the constitutive relationships proposed by Menegotto and Pinto [55] and by Mander et al. [56], respectively. The analyses were conducted considering only the accelerograms consistent with the EC8 spectra (the suites plotted in Figure 8). NLTHAs were carried out under full-length and short length accelerograms. To validate the procedure, two variables of the seismic response of the archetype have been investigated as target parameters: the horizontal displacement of the center of gravity of the roof level (defined by the connection of the central column and the beam at this level) and the total shear force at the base. For each analysis, the maximum values of roof displacement and total shear at the base were obtained. The absolute difference between the values of such parameters calculated under full-length and short length accelerograms was obtained. This difference (in %) and the mean value over the seven earthquakes are provided in Table 11. It can be noted that EC8, like other codes, advocates working with mean values instead of considering maximum values whenever more than three accelerograms are considered for the analysis.

The results indicate that the differences between the values obtained with full-length and short length accelerograms are relatively small. The maximum difference between the roof displacements is 10.5% (reached for accelerogram 2 and soil type C). The maximum difference between the shear forces is 12.8% (reached for accelerogram 4 and soil type E). However, it is worth noting the arithmetic mean of the calculated differences does not exceed 5% either for displacements or for base shear (see "Mean" columns of Table 11). This validates the effectiveness of the procedure, at least for the kind of structure and the earthquakes considered here.

All the accelerograms given in Figures 7 and 9 have been processed according to the above suggested procedure and the corresponding short length accelerograms have been obtained. They can be freely downloaded from a repository hosting them, as indicated at the end of the paper. It is worth noting that, on average, the short-length EC8 and IBC

consistent accelerograms are found to be, respectively, about 1/5 and 1/4 of the full-length ones, although much stronger reductions are achieved for some of the accelerograms. This time-length shortening can drastically reduce the computational time, particularly when non-linear analyses of three-dimensional structures are involved. Some of the short-length IBC-spectrum-consistent earthquakes were successfully used to carry out NLTHAs on a Lebanese historical hammam and predict its post-elastic seismic behavior [57].

Table 11. Summary of the results of the non-linear time-history analyses.

Ground Type	X Acceler.	Roof Displacements		Total Base Shear	
		Abs. Diff. (%)	Mean (%)	Abs. Diff. (%)	Mean (%)
A	1	4.8	3.6	3.7	4.3
	2	3.4		3.6	
	3	1.9		2.9	
	4	2.9		3.4	
	5	7.8		2.3	
	6	2.2		5.7	
	7	2.3		8.8	
B	1	3.3	4.1	3.4	3.9
	2	9.6		5.0	
	3	1.9		2.9	
	4	3.2		2.5	
	5	1.5		1.6	
	6	5.3		7.5	
	7	3.8		4.3	
C	1	1.7	4.7	0.1	4.1
	2	10.5		4.9	
	3	2.1		2.8	
	4	9.9		11.4	
	5	0.8		3.5	
	6	4.3		1.9	
	7	3.8		4.3	
D	1	3.3	4.6	3.5	3.3
	2	1.5		7.0	
	3	5.2		4.0	
	4	5.8		1.5	
	5	5.8		2.7	
	6	9.9		3.7	
	7	0.4		0.7	
E	1	1.4	4.6	5.9	4.9
	2	9.3		1.0	
	3	6.9		2.4	
	4	2.7		12.8	
	5	5.1		10.6	
	6	1.4		1.0	
	7	5.7		0.4	

8. Comparing the Seismic Demand Obtained from the Different Codes

A comparison is presented in this section to check the consequences of adopting one or the other of the four different codes referred to by the Lebanese standard, namely PS-92, UBC, IBC and EC8. For this purpose, a series of linear analyses have been conducted on the same archetype given in Figure 11, the fundamental period of which is T = 0.39 s. This allows for an objective weighting of the demand imposed on a structure with a fundamental period that typically places acceleration demands on the plateau of the design spectra (or in its vicinity), thereby allowing seismic demands to be high. Firstly, MRSAs on the archetype have been performed, with reference to the elastic spectra given by the four codes and to the

categories of site/soil A, B, C, D and E. The two variables assessed are roof displacements and base shear force.

The results obtained through the MRSAs for the different codes are presented in Figure 12. Both topographical factors $\tau = 1$ and $\tau = 1.4$ are considered for the PS92 spectra. Figure 12 shows that, in general, and as expected, soft soils impose higher displacement and force demands. Some exceptions are found for S2 and S3 soils when referring to the PS92 standard, and for E soils and C soils when referring to IBC and EC8 spectra, respectively. For very stiff soils (PS92-S0, UBC-SA, IBC-SA, and EC8-SA), the values of the roof displacement are relatively uniform between the different codes, with a maximum difference of 31.09% between the highest (EC8-SA) and the lowest (PS92-S0, $\tau = 1$) values. For very soft soils (PS92-S3, UBC-SE, IBC-SE, and EC8-SE), the highest difference (89.05%) is observed once again between the results relevant to PS-92 ($\tau = 1$) and EC8 (see Figure 12a). Similarly, when the base shear force is concerned, a maximum difference of 31.52% and of 90% was found, respectively, for very stiff soils and for soft soils between PS92 ($\tau = 1$) and EC8.

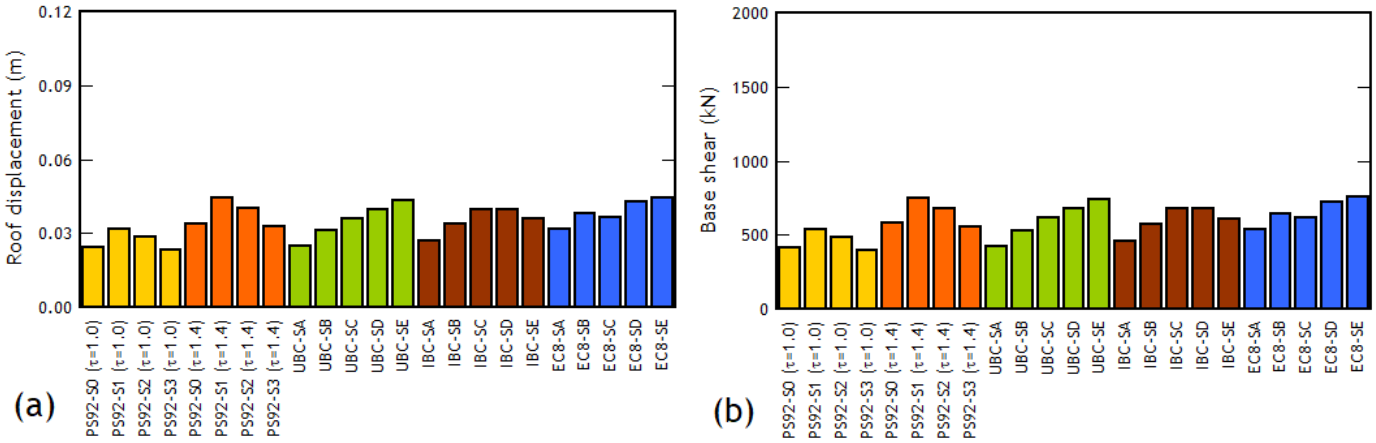

Figure 12. (**a**) Roof displacements and (**b**) base shear calculated through MRSAs with reference to the different codes.

When a topographic factor $\tau = 1.4$ is considered in the PS92 spectra, the difference between the roof displacements obtained with EC8 and PS92 lowers to 6.29% for very stiff soils and to 35.03% for soft soils. Similarly, the difference between base shear forces lowers to 6.77% for very stiff soils and to 35.55% for soft soils. It should be noted, however, that $\tau = 1.4$ is the maximum value of the topographical factor, provided by PS92 for very high slopes of the site. On the other hand, no topographical factor is introduced by the other considered codes. This leads to an inconsistency in the present comparison and, above all, in the Lebanese design.

LTHAs have also been conducted using the seven EC8-spectrum-consistent accelerograms. Figure 13a presents the results obtained for the maximum roof displacements. It is noteworthy that the values of displacements calculated through LTHAs are higher than those obtained through MRSAs, which is typical when comparing these two types of analyses [8]. Similarly, the results of the maximum calculated values of base shear forces for the seven accelerograms compatible with EC8 spectra are shown in Figure 13b. Once again, an increase in the values is observed as the soils become softer.

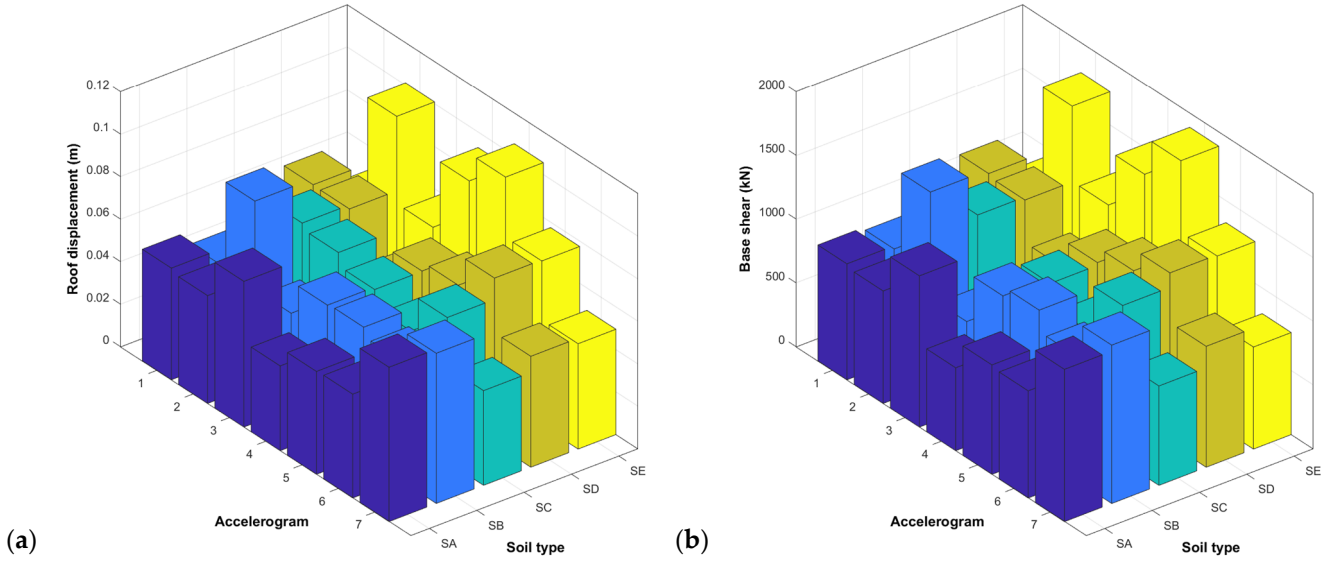

Figure 13. (**a**) Roof displacements and (**b**) base shear forces, calculated through LTHAs under the accelerograms generated for EC8.

9. Conclusions

This paper highlights some issues that are affecting the Lebanese seismic design and gives hints and tools to suitably address them. A main issue is related to the excess of design response spectra that are admitted by the Lebanese code, which may create confusion in civil engineering practice. Another issue is the reference that is made to foreign codes that conflict with each other and/or are not mandatory anymore in their countries. A correlated issue concerns the difficulty to get all the parameters that are needed to obtain the Lebanese design response spectra by following the indications of such foreign codes. In addition to the ambiguity of the design response spectra to be adopted, there are also matters related to the scarcity of recorded earthquakes in the Lebanese area which makes it difficult to obtain suitable suites of spectrum-consistent earthquakes to carry out transient analyses. Finally, even when appropriate spectrum-consistent earthquakes are found, their excessive length may be a further cumbersome problem.

Sorting through the four codes indicated by the Lebanese code and the applicative instructions given for each of them, this paper provides all the design response spectra that can be used for the Lebanese design. This tidying up job, which was not fully completed before, led to supply formulas, tables of parameters and graphs that can be very useful for Lebanese practitioners. The comparison evidenced the differences between the many design spectra that are indistinctly admitted by the Lebanese code which is thus found to implicitly admit different safety levels for similar buildings grounded on the same soil class. The comparative study also showed that the topographical effects are not accounted for in most of the design spectra, the only code providing topographical factors being the obsolete French code. This may add further inconsistencies to the seismic design, as showed by the comparison of the results. Although the aim of this paper is obviously far from giving specific design instructions, this matter being the responsibility of the Lebanese Government, the use of two codes that are currently in force (among the four referred to) is suggested in this paper, namely the International Building Code (IBC) and the Eurocode 8 (EC8). The first one is the official seismic code in the USA as well as a reference code in many other countries, like Chile. The second one is the reference code for many of the European countries and it is even announced to be the only future reference code in Lebanon. When EC8 is the Lebanese reference code, it is suggested to also provide topographical factors to obtain different design response spectra for different topographical conditions, as it is done, for instance, by the Italian code.

To address the matter of lack of proper accelerograms to be used for the seismic assessment of the Lebanese structures through time-history analyses, wide research in many seismic databases was carried out which eventually led to finding some strong earthquakes that occurred along the Dead Sea Transform Fault. Those records were assumed to be seismogenically representative of the seismic events occurring in Lebanon. By elaborating them, both in the time and in the frequency domain, suitable sets of accelerograms that are consistent with the design response spectra of IBC and of EC8 are found for the different considered soil categories. The synthetization process was carried out through a spectral matching method by considering a 10% upper and lower mismatch tolerance.

Since the time length of such accelerograms is typically rather long, which implies a large computational burden, the matter of shortening the spectrum-consistent accelerograms was also addressed in the paper. Based on the Arias intensity of a given earthquake, a procedure is proposed, which can be implemented with the help of commercial matching tools. This procedure was shown to drastically reduce the duration of the horizontal components of a given earthquake while saving 95% of its energy content. On average, the short-length EC8- and IBC-consistent accelerograms are found to be, respectively, about 1/5 and 1/4 of the full-length ones. The effectiveness of the procedure was validated by applying full-length and short length accelerograms to a 2D archetype building and comparing some key parameters. On average, an error less than 5% was found which shows the effectiveness of the procedure, at least for the type of building and the suites of earthquakes considered. Wider future investigation of 3D models of various structural typologies under earthquakes from other seismic regions is needed to definitively validate the general efficacy of the proposed procedure. As obtained from this procedure, the corresponding ten suites of short length accelerograms are made freely downloadable from the repository. They can be profitably exploited to reduce the burden of linear and non-linear time-history analyses of Lebanese structures, while saving the effectiveness of the results.

By referring to an archetype building, linear response-spectrum-based and earthquake-based analyses are finally carried out to highlight the different levels of safety allowed by the Lebanese code. The results reveal that the various international codes considered for design in Lebanon exhibit comparatively consistent values for very stiff soils, with a maximum difference slightly exceeding 30%. However, for soft soils, this difference increases to values approaching even 90% when the lowest topographical factor is assumed for the French spectra. In pursuit of an appropriate seismic-resistant design, it is recommended to employ the spectra of EC8 and its corresponding accelerograms, as they yield higher demand values for both displacements and base shear forces with respect to the other considered codes.

The data and the tools provided, together with the examples discussed, make the content of this paper of great impact for the seismic design/assessment of new/existing structures in Lebanon, thus significatively contributing to the seismic protection of the Lebanese building heritage. On the other hand, the highly promising procedure to reduce the accelerogram length could be exploited to expedite the non-linear time-history analyses of buildings in any other earthquake-prone country.

Author Contributions: Conceptualization, M.C.P. and J.C.V.P.; methodology, A.G., M.C.P. and J.C.V.P.; software, A.G.; validation, A.G. and J.C.V.P.; formal analysis, A.G. and M.C.P.; investigation, A.G., M.C.P. and J.C.V.P.; data curation, A.G.; writing—original draft preparation, M.C.P. and J.C.V.P.; writing—review and editing, M.C.P. and J.C.V.P.; visualization and supervision, M.C.P. and J.C.V.P. All authors have read and agreed to the published version of the manuscript.

Funding: The financial support of Fondazione di Sardegna through the grant Surveying, modelling, monitoring and rehabilitation of masonry vaults and domes (Rilievo, modellazione, monitoraggio e risanamento di volte e cupole in muratura—RMMR, CUP code: F72F20000320007) is gratefully acknowledged.

Institutional Review Board Statement: Not applicable.

Informed Consent Statement: Not applicable.

Data Availability Statement: The data of all the full-length and short-length earthquakes consistent with the IBC and EC8 spectra is available in Google Drive at https://drive.google.com/drive/folders/1HNi1v3cyaj3iAoxijJ5tC5jhGRm1072v?usp=drive_link0 (accessed on 2 September 2023).

Acknowledgments: The 2020 Visiting Professors program of the University of Cagliari is acknowledged. This research has been developed for the partial fulfillment of the doctoral program of A.G. at Scuola di Dottorato in Ingegneria Civile e Architettura, University of Cagliari. The authors wish to thank the Pontificia Universidad Católica de Valparaíso for financing the publication of this paper.

Conflicts of Interest: The authors declare no conflict of interest.

References

1. Paglietti, A.; Porcu, M.C.; Pittaluga, M. A loophole in the Eurocode 8 allowing for non-conservative seismic design. *Eng. Struct.* **2011**, *33*, 780–785. [CrossRef]
2. Krawinkler, H.; Seneviratna, G.D.P.K. Pros and cons of a pushover analysis of seismic performance evaluation. *Eng. Struct.* **1998**, *20*, 452–464. [CrossRef]
3. Vielma-Perez, J.; Porcu, M.C.; Gómez, M. Non-linear analyses to assess the seismic performance of RC buildings retrofitted with FRP. *Rev. Int. Metodos Numer. Calc. Diseno Ing.* **2020**, *36*, 1–13. [CrossRef]
4. Gerges, A.; Fares, N. Feasibility of the underground earthquake bracelet. In *Computational Methods and Experimental Measurements XIX & Earthquake Resistant Engineering Structures XII*; WIT Press: Boston, MA, USA, 2019; Volume 125, pp. 109–120.
5. Porcu, M.C.; Bosu, C.; Gavrić, I. Non-linear dynamic analysis to assess the seismic performance of cross-laminated timber structures. *J. Build. Eng.* **2018**, *19*, 480–493. [CrossRef]
6. Porcu, M.C.; Vielma, J.C.; Panu, F.; Aguilar, C.; Curreli, G. Seismic retrofit of existing buildings led by non-linear dynamic analyses. *Int. J. Saf. Secur. Eng.* **2019**, *9*, 201–212. [CrossRef]
7. Vielma, J.C.; Porcu, M.C.; López, N. Intensity Measure Based on a Smooth Inelastic Peak Period for a More Effective Incremental Dynamic Analysis. *Appl. Sci.* **2020**, *10*, 8632. [CrossRef]
8. Porcu, M.C.; Vielma Pérez, J.C.; Pais, G.; Osorio Bravo, D.; Vielma Quintero, J.C. Some Issues in the Seismic Assessment of Shear-Wall Buildings through Code-Compliant Dynamic Analyses. *Buildings* **2022**, *12*, 694. [CrossRef]
9. Porcu, M.C. Code inadequacies discouraging the earthquake-based seismic analysis of buildings. *Int. J. Saf. Secur. Eng.* **2017**, *7*, 545–556.
10. Abdul-Wahed, M.K.; Asfahani, J. New insight on the recent instrumental seismic activity along the Serghaya fault, Syria. *Geofis. Int.* **2017**, *56*, 243–253.
11. Nemer, T.; Meghraoui, M.; Khair, K. The Rachaya-Serghaya fault system (Lebanon): Evidence of coseismic ruptures, and the AD 1759 earthquake sequence. *J. Geophys. Res. Solid Earth* **2008**, *113*, B05312. [CrossRef]
12. Tabbara, M.R.; Karam, G.K. The use of numerical methods to investigate the seismic response of a large block masonry colonnade. In Proceedings of the 9th US National & 10th Canadian Conference on Earthquake Engineering (9USN/10CCEE): Reaching Beyond Borders, Toronto, ON, Canada, 25–29 July 2010. Paper No 466.
13. Iervolino, I.; Galasso, C.; Cosenza, E. REXEL: Computer-aided record selection for code-based seismic structural analysis. *Bull. Earthq. Eng.* **2010**, *8*, 339–362. [CrossRef]
14. Kayhan, A.H.; Demir, A.; Palanci, M. Statistical evaluation of maximum displacement demands of SDOF systems by code-compatible nonlinear time history analysis. *Soil Dyn. Earthq. Eng.* **2018**, *115*, 513–530. [CrossRef]
15. Demir, A.; Palanci, M.; Kayhan, A.H. Evaluation of Supplementary Constraints on Dispersion of EDPs Using Real Ground Motion Record Sets. *Arab. J. Sci. Eng.* **2020**, *45*, 8379–8401. [CrossRef]
16. Palanci, M.; Demir, A.; Kayhan, A.H. Quantifying the effect of amplitude scaling of real ground motions based on structural responses of vertically irregular and regular RC frames. *Structures* **2023**, *51*, 105–123. [CrossRef]
17. Demir, A.; Kayhan, A.H.; Palanci, M. Response- and probability-based evaluation of spectrally matched ground motion selection strategies for bi-directional dynamic analysis of low- to mid-rise RC buildings. *Structures* **2023**, *58*, 105533. [CrossRef]
18. Demir, A.; Palanci, M.; Kayhan, A.H. Evaluation the effect of amplitude scaling of real ground motions on seismic demands accounting different structural characteristics and soil classes. *Bull. Earthq. Eng.* **2023**. [CrossRef]
19. Brax, M.; Causse, M.; Bard, P.-Y. Ground motion prediction in Beirut: A multi-step procedure coupling empirical Green's functions, ground motion prediction equations, and instrumental transfer functions. *Bull. Earthq. Eng.* **2016**, *14*, 3317–3341. [CrossRef]
20. Arango, M.C.; Lubkowski, Z.A. Seismic hazard assessment and design requirements for Beirut, Lebanon. In Proceedings of the 15th World Conference in Earthquake Engineering, Lisbon, Portugal, 28 September 2012.
21. Trifunac, M.D.; Brady, A.G. A study on the duration of strong earthquake ground motion. *Bull. Seismol. Soc. Am.* **1975**, *65*, 581–626.
22. Zhong, P.; Zareian, F. Method of speeding up buildings time history analysis by using appropriate downsampled integration time step. In Proceedings of the 10th US National Conf. on Earthquake Engineering, Oakland, CA, USA, 21–25 July 2014.

23. Reyes, J.C.; Avila, W.A.; Kalkan, E.; Sierra, A. Reducing Processing Time of Nonlinear Analysis of Symmetric-Plan Buildings. *J. Struct. Eng.* **2021**, *147*, 04021073. [CrossRef]
24. Girdler, R.W. The Dead Sea transform fault system. *Tectonophysics* **1990**, *180*, 1–13. [CrossRef]
25. Khair, K. Geomorphology and seismicity of the Roum fault as one of the active branches of the Dead Sea fault system in Lebanon. *J. Geophys. Res. Solid Earth* **2001**, *106*, 4233–4245. [CrossRef]
26. Wdowinski, S.; Bock, Y.; Baer, G.; Prawirodirdjo, L.; Bechor, N.; Naaman, S.; Knafo, R.; Forrai, Y.; Melzer, Y. GPS measurements of current crustal movements along the Dead Sea Fault. *J. Geophys. Res. Solid Earth* **2004**, *109*, B05403. [CrossRef]
27. Brax, M.; Albini, P.; Beauval, C.; Jomaa, R.; Sursock, A. An Earthquake Catalog for the Lebanese Region. *Seismol. Res. Lett.* **2019**, *90*, 2236–2249. [CrossRef]
28. Nemer, T.; Meghraoui, M. Evidence of coseismic ruptures along the Roum fault (Lebanon): A possible source for the AD 1837 earthquake. *J. Struct. Geol.* **2006**, *28*, 1483–1495. [CrossRef]
29. Meirova, T.; Hofstetter, R. Observations of seismic activity in Southern Lebanon. *J. Seismol.* **2013**, *17*, 629–644. [CrossRef]
30. Salamon, A. Patterns of seismic sequences in the Levant—Interpretation of historical seismicity. *J. Seismol.* **2010**, *14*, 339–367. [CrossRef]
31. *NL135*; NL:135. Ministry of Industry. The Lebanese Standards Institution (LIBNOR): Beirut, Lebanon, 2012.
32. *PS92*; Règles PS Applicables aux Bâtiments, Dites Règles PS92. NF P 06-013/DTU Règles PS92. AFNOR: Paris, France, 1995.
33. UBC. Uniform Building Code. In Proceedings of the International Conference of Building Officials, Whittier, CA, USA; 1997.
34. IBC. *International Building Code*; Ch.16 S.13 Earthquake Loads; International Code Council: Washington, DC, USA, 1997.
35. *EC8*; CEN European Standard ENV 1998-1-1/2/3, Eurocode 8: Design Provisions for Earthquake Resistance of Structures—Part I: General Rules. Technical Committee 250/SC8. Technical Committee: Brussels, Belgium, 2004.
36. Valdés-Vázquez, J.-G.; García-Soto, A.D.; Jaimes, M.Á. Impact of the Vertical Component of Earthquake Ground Motion in the Performance Level of Steel Buildings. *Appl. Sci.* **2021**, *11*, 1925. [CrossRef]
37. Negrisoli, G.; O'Connor, M.; Xavier, F. Performance-based seismic design: Challenges of application for a tall building in a high seismic zone. In Proceedings of the 6th World Conference on Earthquake Engineering, Santiago, Chile, 9–13 January 2017; Paper No 2297.
38. ESM. Engineering Strong Motion Database. Available online: https://esm-db.eu/#/home (accessed on 2 November 2022).
39. COSMOS. Virtual Data Center. Available online: https://www.strongmotioncenter.org/vdc/scripts/default.plx (accessed on 2 November 2022).
40. *ASCE 7-16*; Minimum Design Loads and Associated Criteria for Buildings and Other Structures. American Society of Civil Engineers: Reston, VA, USA, 2016.
41. Hancock, J. An improved method of matching response spectra of recorded earthquake ground motion using wavelets. *J. Earthq. Eng.* **2006**, *10*, 67–89. [CrossRef]
42. Hancock, J.; Bommer, J.J.; Stafford, P.J. Numbers of scaled and matched accelerograms required for inelastic dynamic analyses. *Earthq. Eng. Struct. Dyn.* **2008**, *37*, 1585–1607. [CrossRef]
43. Léger, P.; Tayebi, A.K.; Paultre, P. Spectrum-compatible accelerograms for inelastic seismic analysis of short-period structures located in eastern Canada. *Can. J. Civ. Eng.* **1993**, *20*, 951–968. [CrossRef]
44. Kaul, M.K. Spectrum-Consistent Time-History Generation. *J. Eng. Mech. Div.* **1978**, *104*, 781–788. [CrossRef]
45. Lilhanand, K.; Tseng, W.S. Generation of synthetic time histories compatible with multiple-damping response spectra. In Proceedings of the Transactions of the 9th International Conference on Structural Mechanics in Reactor Technology, Lausanne, Switzerland, 17–21 August 1987; pp. 105–112.
46. Lilhanand, K.; Tseng, W.S. Development and application of realistic earthquake time histories compatible with multiple damping response spectra. In Proceedings of the Ninth World Conference on Earthquake Engineering, Tokyo, Japan, 2 August 1988; pp. 819–824.
47. Abrahamson, N.A. Non-stationary spectral matching. *Seism. Res Lett.* **1992**, *63*, 30.
48. SeismoMatch. A Computer Program for Spectrum Matching of Earthquake Records. Seismosoft. 2016. Available online: https://www.seismosoft.com (accessed on 1 January 2023).
49. *FEMA P-1050*; NEHRP Recommended Seismic Provisions for New Buildings and Other Structures. Building Seismic Safety Council: Washington, DC, USA, 2015.
50. Baker, J.W.; Haselton, C.B.; Luco, N.; Stewart, J.P.; Zimmerman, R.B. Updated ground motion spectral matching requirements in the 2015 NEHRP recommended seismic provisions. In Proceedings of the 6th International Conference on Earthquake Geotechnical Engineering, Christchurch, New Zealand, 1–4 November 2015.
51. *NTC2008*; New Technical Norms on Constructions, GU n.29 04/02/2008. Ministry of Public Works: Rome, Italy, 2008.
52. Arias, A. A Measure of Earthquake Intensity. In *Seismic Design for Nuclear Power Plants*, 1st ed.; Hansen, R.J., Ed.; MIT Press: Cambridge, MA, USA, 1970.
53. SeismoSignal. A Computer Program for Signal Processing of Time-Histories. Seismosoft. 2016. Available online: https://www.seismosoft.com (accessed on 1 January 2023).
54. Frau, C.; Panella, S.; Tornello, M. Input Energy Spectra for Pulse-Like Ground Motions. In Proceedings of the International Workshop on Energy-Based Seismic Engineering, Porto, Portugal, 3–6 July 2023; pp. 216–233.

55. Menegotto, M.; Pinto, P.E. Plane Frame Including Changes in Geometry and Non-Elastic Behaviour of Elements under Combined Normal Force and Bending. In Proceedings of the IABSE Symposium on Resistance and Ultimate Deformability of Structures Acted on by Well Defined Repeated Loads, Lisbon, Portugal, 15–22 January 1973; pp. 15–22.
56. Mander, J.B.; Priestley, M.J.; Park, R. Theoretical stress-strain model for confined concrete. *J. Struct. Eng.* **1998**, *114*, 1804–1826. [CrossRef]
57. Gerges, A.; Porcu, M.C.; Cazzani, A. Numerical investigation of the post-elastic seismic response of the multi-vaulted Beit-El-Din Hammam. *Int. J. Mason. Res. Innov.* **2023**, *1*, 10058266. [CrossRef]